Cure of human carcinoma xenografts by a single dose of pretargeted yttrium-90 with negligible toxicity

D. B. Axworthy*, J. M. Reno, M. D. Hylarides, R. W. Mallett, L. J. Theodore, L. M. Gustavson, F.-M. Su, L. J. Hobson, P. L. Beaumier, and A. R. Fritzberg

NeoRx Corporation, Seattle, WA 98119

Communicated by M. Frederick Hawthorne, University of California, Los Angeles, CA, October 25, 1999 (received for review June 21, 1999)

A covalent conjugate (NR-LU-10/SA) was prepared between streptavidin (SA) and NR-LU-10, a mAb that binds an antigen expressed on the surface of most human carcinomas. NR-LU-10/SA was injected into nude mice bearing human tumor xenografts. Injection of biotinylated galactosyl-human serum albumin reduced the circulating levels of conjugate by 95%. Subsequent administration of ^{90}Y-1,4,7,10-tetraazacyclododecane-1,4,7,10-tetraacetic acid-biotin achieved peak uptake at the tumor within 2 hr while >80% of the radioactivity was eliminated in the urine. A single dose of 600–800 μCi of ^{90}Y-1,4,7,10-tetraazacyclododecane-1,4,7,10-tetraacetic acid-biotin produced cures in 10/10 mice with established (>200 mm^3) s.c. human small cell lung or colon cancer xenografts and 8/10 cures in mice with human breast cancer xenografts without significant toxicity.

Despite its proven efficacy in the treatment of cancer, external beam radiotherapy often is used for locally advanced disease at confirmed sites and can be limited to suboptimal doses because of normal tissue exposure within the radiation field. Radioimmunotherapy (RIT), targeting radiation to tumor by using β-emitting radioisotopes conjugated to a mAb, has been proposed to achieve specific and efficient delivery of cytotoxic radiation to systemic metastases while sparing exposure to normal tissues (1). Antibodies directed to tumor-associated antigens seem fitting targeting vehicles for site-specific delivery of radiation to tumors. Furthermore, radiation appears to be a suitable cytotoxic agent in that it can exert its damaging effects not only to the cell on which it is bound, but also to neighboring cells within the tumor. In contrast, toxin- or drug-mAb conjugates must bind to tumor cells, be internalized, and release sufficient concentrations of active molecules to exert cytotoxicity (2, 3).

Despite occasional positive results in preclinical models, RIT has failed to achieve reproducible clinical efficacy in carcinomas (4), because of several factors. Carcinomas present physiologic and structural barriers (e.g., poor and abnormal vascularization and high intratumoral pressure) that limit delivery of pharmacologic agents, particularly high molecular weight molecules such as whole antibodies (5). Second, peak tumor uptake of antibody may not occur until 24–48 hr after injection, whereas serum half-lives of $\geq$24 hr prolong radiation exposure to normal organs and radiosensitive bone marrow, which limits the radiation dose that can be safely administered (6). Third, relatively low and heterogeneous tumor uptake can be a result of low or nonuniform antigen expression by tumor cells (7). Finally, β-emitting radioisotopes deliver low-dose rate radiation that, at low concentrations, may be insufficient to overcome the continual proliferation and repair of solid tumor cells. Appropriate choice of an antigenic target and increased mass dose of antibody can address antibody penetration and heterogeneity limitations. In the context of RIT, however, increasing the amount of carrier antibody also can serve to dilute the potency and delivery efficiency of the radioisotope into solid tumors. The slow accretion of whole antibody into carcinomas exacerbates the progressive loss of potency caused by radioisotope decay, limiting effective utilization of short-lived, high-energy radionuclides, such as ^{90}Y. Generally, clinical application of RIT to solid tumor indications has failed to deliver sufficient radiation dose to tumors, primarily because of dose-limiting radiation exposure to bone marrow (8).

To overcome some of the obstacles encountered by conventional RIT, antibody and radionuclide can be injected separately, effectively decoupling the pharmacokinetics of the radionuclide from the antibody. Several multistep strategies have been described (9–12). The approach described here uses the tumor targeting specificity of the antibody to carry a receptor that can bind a subsequently administered low molecular weight ligand, chemically modified to stably chelate a radioisotope. This method permits high, antigen-saturating doses of antibody-receptor conjugate to be safely administered. The time interval allowed to elapse between injection of this antibody-receptor conjugate and injection of the radioisotope-ligand accommodates the aforementioned pharmacokinetic constraints of antibody localization into carcinomas. Formulating the radioisotope as a small molecule ligand results in rapid extravasation into tumor interstitial fluid. We chose biotin-streptavidin (SA) as the receptor-ligand pair, to ensure ligand binding with high affinity to the tumor-localized antibody-receptor conjugate. The excess low molecular weight radioactivity is rapidly eliminated from the body via renal elimination. Because of this short whole-body residence time, higher doses of radioactivity can be administered.

One approach, called pretargeting by Goodwin and Meares *et al*. (13, 14), also uses an intermediate clearing step in which nontarget bound antibody conjugate is specifically removed from circulation before radioisotope administration (to minimize the fraction that can bind to circulating conjugate). We have compared our version of pretargeting to conventional RIT as assessed by radiolabel biodistribution, tumor delivery efficiency, toxicity, and therapeutic efficacy in relevant human tumor xenograft models. We report here a system that addresses the limitations of conventional RIT, permits safe, systemic administration of high doses of radioactivity, and produces cures in a variety of established tumor xenografts with only a single treatment.

Materials and Methods

NR-LU-10/SA Conjugate. Murine IgG$_{2b}$ mAb NR-LU-10 recognizes a 40-kDa epithelial antigen known as Ep-CAM (15, 16). This antibody has been studied both in animals and in human clinical trials (17, 18). NR-LU-10 was chemically conjugated to SA (Genzyme) by using succinimidyl 4-(*N*-maleimido-methyl) cyclohexane-1-carboxylate (SMCC). Excess SMCC was offered

Abbreviations: SA, streptavidin; RIT, radioimmunotherapy; DOTA, 1,4,7,10-tetraazacyclododecane-1,4,7,10-tetraacetic acid; HSA, human serum albumin; i.d., injected dose; CA, clearing agent; MTD, maximum tolerable dose; AUC, area under curve.

*To whom reprint requests should be addressed at: 410 West Harrison Street, Seattle, WA 98119. E-mail: daxworthy@neorx.com.

The publication costs of this article were defrayed in part by page charge payment. This article must therefore be hereby marked "*advertisement*" in accordance with 18 U.S.C. §1734 solely to indicate this fact.

to SA in a 3:1 molar ratio in sodium borate at pH 8 containing 5% DMSO. After 30 min, the SMCC-SA was desalted by Sephadex G-25 (Amersham Pharmacia) gel filtration. NR-LU-10 was reduced with DTT, desalted by gel filtration and mixed in 1:1 molar ratio with SMCC-SA at 5 mg/ml total protein concentration in PBS. The reaction was monitored by size exclusion HPLC, and after sufficient conjugate had formed, *ca.* 50 min, the reaction was quenched by the addition of sodium tetrathionate to 5 mM to reoxidize unreacted thiols. The conjugate was separated from free SA by Q Sepharose chromatography. The conjugate was applied to a column equilibrated in 0.05 M sodium phosphate, pH 7.8 and eluted in the same buffer containing 0.2 M sodium chloride. The conjugate was separated from unconjugated antibody by affinity chromatography using immobilized iminobiotin (Pierce) equilibrated in 0.05 M sodium carbonate, 0.5 M sodium chloride, pH 11 and eluting with 0.05 M sodium acetate/0.5 M sodium chloride, pH 4. The conjugate appears as a single peak on size exclusion HPLC with UV detection. By SDS/PAGE, about 80% of the conjugate consists of SA/antibody in a 1:1 ratio, with the remainder primarily in a 2:1 ratio or higher. Immunoreactivity of the conjugate was 90% of unconjugated antibody as assessed by an ELISA (19). The biotin binding capacity of the conjugate, as determined by 2-(4′-hydoxyphenylazo)-benzoic acid (HABA) displacement from SA by biotin (20), was calculated to be 4.5 moles biotin per mole conjugate, reflecting the presence of a small percentage of antibody conjugated to two SA molecules.

^{125}I/^{131}I Radiolabeling. NR-LU-10, SA, and NR-LU-10/SA were radiolabeled by using succinimidyl para-iodobenzoate reagent (21).

^{90}Y-1,4,7,10-Tetraazacyclododecane-1,4,7,10-Tetraacetic Acid (DOTA)-NR-LU-10. NR-LU-10 whole antibody was radiolabeled with ^{90}Y by the preformed chelate method. DOTA-maleimide (4-maleimidobutyramidobenzyl-DOTA) was prepared by the reaction of aminobenzyl-DOTA with 4-maleimidobutyric acid (Fluka) activated with isopropylchloroformate (Aldrich). Carrier free $^{90}YCl_3$, 10 mCi in 0.01 ml of 0.05 M HCl (DuPont) was diluted with 0.1 ml of 0.5 M sodium acetate, pH 5. Forty micrograms of DOTA-maleimide was added, and the solution was heated at 75°C for 45 min to yield the preformed chelate. NR-LU-10 was reduced with DTT, desalted over Sephadex G-10, and reacted with ^{90}Y-DOTA-maleimide in PBS at room temperature for 15 min. The radiolabeled protein was purified over Sephadex G-10 in PBS. Specific activity ranged from 1 to 4 μCi·μg^{-1}. Immunoreactivity (assessed by cell binding, ref. 17) was >80%.

Biotin-Galactose-Human Serum Albumin (HSA). HSA was reacted with 3-fold excess *N*-hydroxysuccinimide-LC-biotin (Pierce) in 0.5 M sodium borate (pH 8.5), 5% DMSO. After *ca.* 4 hr the solution was added to a 200-fold excess of freshly prepared neat 2-imino-2-methoxyethyl 1-thio-β-D-galactopyranoside (22). The mixture was stirred for 8 hr at room temperature and purified by diafiltration into PBS. The final material contained 1.6 moles of biotin per mole of HSA as determined by displacement of 2-(4′-hydoxyphenylazo)-benzoic acid (HABA) from SA and 30–40 moles of thiogalactose per mole of HSA as determined by a colorimetric anthrone assay (23).

^{111}In-DOTA-Biotin. The bifunctional ligand DOTA-biotin was synthesized as described (24). Carrier-free $^{111}InCl_3$, 0.02–0.5 ml in 0.04 M HCl (Amersham Pharmacia), was diluted with 0.5 ml of 2 M ammonium acetate pH 5. DOTA-biotin, 0.1–1 mg, was added, and the solution was heated for 1 hr at 80°C. Diethylenetriaminepentaacetic acid (DTPA) was added to chelate any unbound ^{111}In. Radiochemical purity (>99%) was determined by C_{18} reverse-phase gradient HPLC (A: 5 mM aqueous DTPA, B: 50% acetonitrile in A) with flow-through gamma detection.

^{90}Y-DOTA-Biotin. Carrier-free $^{90}YCl_3$, 0.02–0.2 ml in 0.05 M HCl, was diluted with 2 M ammonium acetate, pH 5 to a total volume of 0.4 ml. Ascorbic acid, 0.05 ml of a 0.5 g/ml solution and 0.1 ml of 10 mg/ml DOTA-biotin, was added, and the solution was heated at 80°C for 1 hr. DTPA, 0.05 ml of a 0.1 M solution was added to chelate any unbound radiometal. Radiochemical purity (>99%) was determined by gradient HPLC with gamma detection as above.

Cell Lines. LS-180 (ATCC CL 187), a human colon adenocarcinoma cell line, was obtained from the American Type Culture Collection. SW1222 human colon adenocarcinoma cells, MDA-MB-484 human breast adenocarcinoma cells, and SHT-1 human small cell lung cancer cells were obtained from the National Cancer Institute, Bethesda, MD.

Mouse Studies. All animal studies were conducted under the supervision of the NeoRx Animal Care and Use Committee. Biodistribution studies were conducted as described (17). Because mice have 10–100 times higher serum concentration of biotin than found in humans (25, 26), they were placed on a biotin-deficient diet (Purina Biotin Deficient Diet 5836, Purina Mills, Richmond, IN) 5 days before study. This time period on the specialized diet resulted in stable serum biotin levels of 0.2–0.4 ng/ml, which are similar to those measured in humans.

Hematopoietic toxicity was assessed in nontumored BALB/c mice. Blood was sampled weekly for analysis of leukocyte and platelet counts. Mouse blood (venous draw) was collected into a Unipet EDTA capillary tube and diluted 1:251 by using a Serano (Geneva, Switzerland) Haemoline diluent silo. Samples were run on a Serano Diagnostics System 9010+ Hematology Analyzer adjusted for mouse hematology analysis. Leukocyte and platelet counts were collected from duplicate samples and the average was reported per mouse.

Tumor Histochemical Analysis. Nude mice bearing LS-180 tumors and maintained on the biotin-free diet were injected with NR-LU-10/SA. At appropriate time points tumors were excised and immediately frozen. To localize SA, tumor sections were blocked with goat serum and overlaid with horseradish peroxidase-conjugated goat anti-SA antibody (Zymed). To localize biotin binding sites, tumor sections were overlaid directly with biotinylated horseradish peroxidase (Vector Laboratories). Detection staining was by 3,3-diaminobenzidine/hydrogen peroxide. Samples were assessed by light microscopy and graded for percent of reactive cells, intensity, and uniformity of staining on a scale of 1–3.

Results

Experimental Approach. This strategy involves the sequential administration of three components, the first and last of which target tumor. The initial step is systemic administration of tumor-selective antibody covalently conjugated to SA (NR-LU-10/SA). The choice of SA as a receptor is based on its extremely high affinity (k_d 10^{-15} M) and specificity for binding the small molecule, biotin, and the rapid kinetics of this interaction (27). SA is commercially available in high purity and has been shown to be stable *in vivo*, retaining its tetrameric structure and ability to bind up to four biotin (or biotin analog) molecules (28), while exhibiting less normal tissue retention than avidin (29). This nontoxic construct slowly accumulates over 24 hr to peak, saturating concentration at tumor antigen-expressing sites. Because of the dose needed for antigenic saturation, a consid-

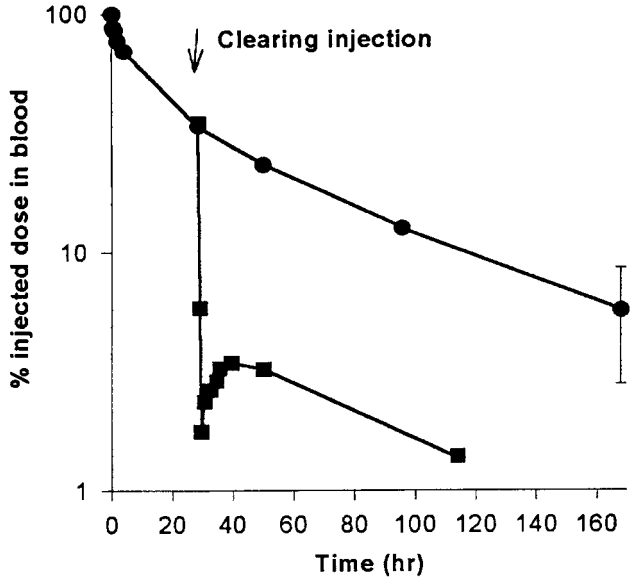

Fig. 1. Effect of CA on blood disappearance *in vivo*. BALB/c mice (n = 3/group) were injected at t = 0 with 400 μg ^{125}I-NR-LU-10/SA conjugate. Blood samples (10 μl, n = 2/time point) were serially removed from the retroorbital plexus and assayed for radioactivity. At 28.5 hr, mice were injected with either saline (●) or 200 μg of CA (■). For the CA mice, blood was sampled at 28.5 (preinjection), 29, 29.5, 30.5, 32.5, 34.5, 35.5, 39.5, 50, and 114 hr. Control animals were sampled at t = 0.17, 0.5, 1.0, 2.0, 4.0, 28.5, 50.0, 72.0, 96.0, and 168 hr. Data are presented as the mean % i.d. in total blood +/− SD of each group.

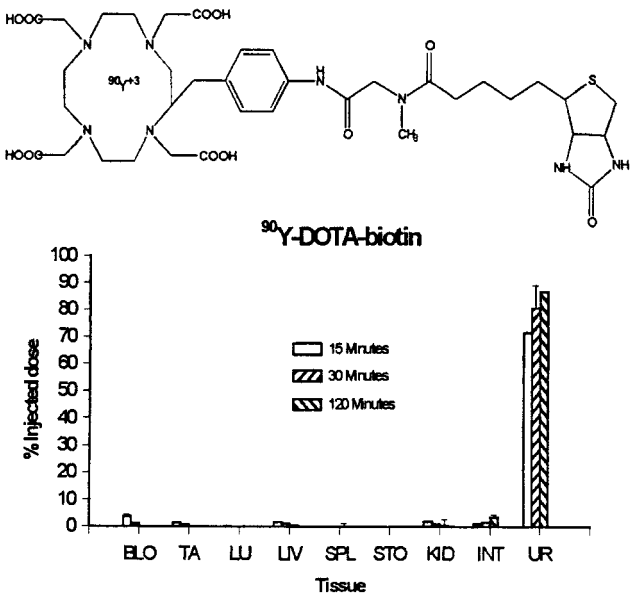

Fig. 2. Structure and biodistribution of ^{90}Y-DOTA-biotin (nonpretargeted). Male BALB/c mice (n = 3/time point) with externally ligated urinary bladders were injected with 5 μg (50 μCi) ^{90}Y-DOTA-biotin. At 15, 30, and 120 min postinjection, blood samples were taken before sacrifice and dissection, and whole organs were assayed for radioactivity. Tissues sampled were (in order) blood, tail, lung, liver, spleen, stomach, kidneys, intestines, and urinary bladder. Data are presented as the mean % i.d. in total blood and each whole organ +/− SD.

erable amount of NR-LU-10/SA remains in circulation. The second component administered is a clearing agent (CA) that rapidly binds to excess circulating NR-LU-10/SA via a biotin moiety and efficiently removes the complex from the blood. This clearance is accomplished through a specific receptor-carbohydrate interaction in the liver, without affecting the tumor-associated NR-LU-10/SA. The final injection is a small (<1 kDa) molecule consisting of a stably chelated cytotoxic radionuclide (^{90}Y) and biotin that can bind specifically and firmly to pretargeted SA at the tumor, while the unbound fraction is rapidly excreted via the urine.

***In Vivo* Performance.** ^{125}I-NR-LU-10/SA was coinjected along with an equimolar amount of ^{131}I-NR-LU-10 antibody into nude mice bearing s.c. LS-180 human colon carcinoma xenografts. Blood clearance and normal organ pharmacokinetics were comparable. Differences in tumor uptake and tumor retention were negligible. Peak tumor uptake of the conjugate was 32.3 ± 6.7% injected dose (i.d.)/g tissue and for the unmodified NR-LU-10 antibody, 36.8 ± 5.6% i.d./g. SA alone (unconjugated to antibody) clears rapidly in mice with blood $t_{1/2}$ <1 hr. At an equimolar dose to NR-LU-10/SA in the same LS-180 xenograft model, the nonantibody targeted tumor uptake of SA is low, with a peak of 2.6 ± 0.5% i.d./g. Additional studies with dual-labeled ^{125}I-NR-LU-10/^{131}I-SA conjugate showed codistribution of each radiolabel, confirming the *in vivo* stability of the conjugate (data not shown).

To establish the appropriate dose of NR-LU-10/SA, nude mice bearing LS-180 tumors were injected with increasing doses, 200–1,000 μg, of conjugate. After 24 and 48 hr, tumors were excised and immediately frozen. Histochemical staining of tumor slices with an anti-SA antibody revealed intense, uniform cell surface reactivity at all doses of conjugate. However, staining with biotinylated horseradish peroxidase showed uniform staining only at injected doses ≥400 μg with qualitatively less staining when tumors were taken at 48 hr versus 24 hr. Although the mice were fed a low-biotin chow diet, this time-dependent loss of biotin binding sites was probably caused by low-level endogenous biotin. All subsequent studies used the 400-μg dose of conjugate.

After injecting 400 μg of NR-LU-10/SA, approximately 30–40% remained in the blood at 24 hr. A CA was designed to remove it from circulation by taking advantage of the galactose receptors present on hepatocytes (30). This receptor is a constitutively recycling unit with a high capacity for trafficking glycoproteins to lysosomes inside heptocytes where they are degraded. The CA, biotin-galactose-HSA, complexes with circulating NR-LU-10/SA through the biotin-SA interaction, and the complex (and excess CA) are removed and degraded by hepatocytes.

Twenty-four hours after i.v. injection of 400 μg of ^{125}I-NR-LU-10/SA, a single injection of 200 μg of CA reduced the amount of conjugate in blood by >90% from 35% i.d. to 1.8% i.d. (Fig. 1) within 2 hr. There was a slight rebound of conjugate from the extravascular compartment back into the blood. Immunohistochemical analysis showed no decrease of biotin binding capacity in tumors pretargeted with NR-LU-10/SA before and after administration of CA at this dose.

After pretargeting of tumor and clearance of circulating conjugate, the cytotoxic radioactive biotin can be given. ^{90}Y [β_{max} = 2.27 MeV, $t_{1/2}$ = 64 hr, X_{90} (the radius of a sphere within which 90% of the energy emitted from a point source is absorbed) = 5.34 mm] was selected as the therapeutic radioisotope because it is a pure, high-energy β-emitter and is commercially available in high specific activity and purity. It is readily complexed by DOTA chelate (31). The structure of DOTA-biotin is shown in Fig. 2. The *N*-methyl amide linker between the DOTA chelate and *d*-biotin is resistant to cleavage by serum biotinidase (24, 32).

^{90}Y-DOTA-biotin diffuses rapidly into a volume of distribution approximately equal to the total extracellular fluid (≈6

Table 1. Comparative biodistributions of ^{125}-NR-LU-10 antibody and pretargeted ^{90}Y-DOTA-biotin

Tissue	^{125}I-NR-LU-10 antibody, percent i.d./g at:				Pretargeted ^{90}Y-DOTA-biotin, percent i.d./g at:			
	2 hr	24 hr	48 hr	120 hr	2 hr	24 hr	48 hr	120 hr
Blood	31.95 (2.88)	18.47 (2.45)	14.70 (0.78)	9.25 (4.02)	1.99 (0.41)	1.22 (0.35)	0.76 (0.22)	0.02 (0.01)
Tail	4.38 (0.60)	3.17 (0.29)	2.71 (0.15)	1.74 (0.42)	0.92 (0.23)	0.65 (0.20)	0.45 (0.11)	0.40 (0.08)
Lung	18.63 (3.24)	13.20 (2.01)	11.16 (1.46)	5.96 (1.85)	1.25 (0.26)	0.76 (0.09)	0.74 (0.29)	0.25 (0.07)
Liver	7.92 (1.19)	3.97 (0.44)	2.48 (0.53)	2.02 (0.40)	0.79 (0.11)	1.03 (0.18)	0.93 (0.18)	0.93 (0.18
Spleen	5.50 (1.50)	4.00 (0.40)	4.41 (0.90)	2.26 (0.61)	0.58 (0.21)	0.61 (0.14)	0.43 (0.05)	0.72 (0.10)
Stomach	2.01 (0.18)	1.24 (0.34)	0.69 (0.09)	0.64 (0.24)	0.35 (0.11)	0.19 (0.07)	0.10 (0.04)	0.06 (0.01)
Kidney	11.14 (1.00)	5.14 (0.56)	4.68 (0.51)	2.79 (0.67)	2.12 (0.25)	2.18 (0.39)	2.45 (0.52)	1.82 (0.21)
Intestine	2.16 (0.41)	2.24 (0.42)	1.19 (0.1)	0.85 (0.28)	1.15 (0.05)	0.37 (0.08)	0.18 (0.03)	0.05 (0.01)
Tumor	9.38 (2.14)	29.94 (6.52)	24.05 (7.79)	18.12 (2.02)	34.96 (6.52)	25.69 (7.70)	22.61 (6.38)	16.69 (1.79)

Data are presented as the mean (SD) of four animals per time point.

ml/25 g mouse). Upon injection into normal mice it is cleared rapidly from the blood through the kidneys with $t_{1/2}$ <15 min. Approximately 90% of the injected dose was excreted intact into the urine by 2 hr and no tissue retained >2% i.d. at 2 hr (Fig. 2).

Several dosing experiments (not shown) were performed to arrive at an optimal protocol: 400 μg (1.905 nmol), i.v. NR-LU-10/SA at $t = 0$, 220 μg (3.143 nmol), i.v. of biotin galactose-HSA at $t = 24$ hr, and 0.3–1.0 μg (0.372–1.239 nmol), i.v. of ^{90}Y-DOTA-biotin at $t = 26$ hr. Using this protocol, the biodistribution of pretargeted ^{90}Y-DOTA-biotin in nude mice bearing SW-1222 human colon carcinoma xenografts was compared with ^{125}I-NR-LU-10 (Table 1). The biodistribution of ^{125}I-NR-LU-10 illustrates the limitations of conventional RIT: protracted blood clearance with accompanying high radiation exposure to normal organs, including radiosensitive bone marrow, and slow uptake into tumor, achieving peak concentrations after 24 hr. In contrast, the biodistribution of pretargeted ^{90}Y-DOTA-biotin showed extremely rapid peak tumor uptake. Subsequent studies showed peak tumor uptake occurred within 15 min after injection. As shown in Table 1, the efficiency of tumor uptake of pretargeted ^{90}Y-DOTA-biotin at 2 hr postinjection was more than three times that of ^{90}Y-whole antibody ($P < 0.01$). From 24 to 120 hr postadministration, tumor uptake of ^{90}Y-DOTA-biotin did not differ significantly from that of ^{90}Y-whole antibody, indicative of comparable tumor retention. Rapid ^{90}Y-DOTA-biotin clearance from blood and tissues minimized radiation exposure to normal organs. Tumor to blood ratios (% i.d. g^{-1} tumor/% i.d. g^{-1} blood) for pretargeted ^{90}Y-DOTA-biotin were 18:1 at 2 hr and >800:1 at 120 hr postinjection. By contrast, the tumor/blood ratios for ^{125}I-NR-LU-10 rarely have exceeded 5:1 by hr postinjection.

In other experiments using ^{111}In-DOTA-biotin (a pure gamma emitter), whole body radiation measurements showed that >80% of the radioactivity administered was cleared from the animals by 2 hr. The high tumor/blood ratios achieved by pretargeted radionuclide reflect a major reduction in nontarget organ radiation exposure when compared with conventional RIT.

Using the data from Table 1, the radiation exposure of tumor and normal tissues was calculated and plotted for ^{90}Y-DOTA-NR-LU-10 (at 200 μCi, the maximum tolerable dose, MTD) and for a high, but less than the MTD, dose of pretargeted ^{90}Y-DOTA-biotin (at 800 μCi). As shown in Fig. 3, the rapid tumor uptake achieved with pretargeting resulted in ≈480% greater tumor dose (area under curve, AUC) and ≈560% higher peak tumor concentration of radionuclide (μCi/g) compared with conventional RIT. Despite the higher initial dose and blood concentration that occurs with pretargeting 800 μCi of ^{90}Y, the total radioactivity exposure in blood was only ≈20% that of conventional. Using the same calculation for equal doses of 200 μCi of ^{90}Y, pretargeting would result in ≈25% greater tumor dose (AUC, μCi/g per hr) and ≈30% higher peak tumor concentration (μCi/g at time of peak uptake) of radionuclide than conventional RIT (at this lower dose, $P = 0.051$).

***In Vivo* Antitumor Activity.** Safety and efficacy of pretargeted ^{90}Y-DOTA-biotin were assessed in therapy studies using nude mice bearing established SW-1222 human colon carcinoma, MDA-MB-484 human breast carcinoma, and SHT-1 human small cell lung carcinoma xenografts. Animal biodistribution studies with NR-LU-10/SA and the other components of pretargeting showed similar results to those described above in each of these tumor types. Treatment consisted of a single dose of pretargeted ^{90}Y-DOTA-biotin, given 10–21 days after tumor cells were implanted and tumors were well established, with volumes between 180 and 300 mm^3. For comparison, each study included one group treated with conventional RIT, ^{90}Y-DOTA-NR-LU-10, given as a single i.v. dose at the MTD of 200 μCi. In the SHT-1 study (Fig. 4*B*), ^{90}Y-DOTA-NR-LU-10 produced some tumor regressions, no cures, and modest growth delay of ≈15 days. By contrast, treatment groups of animals with SHT-1 xenografts receiving 200, 400, or 600 μCi of pretargeted ^{90}Y-DOTA-biotin all had significant tumor regressions. Dose dependency was observed with 7/10 complete tumor regressions at 200 μCi; 9/10, at 400 μCi; and 10/10, at 600 μCi. Cures, defined

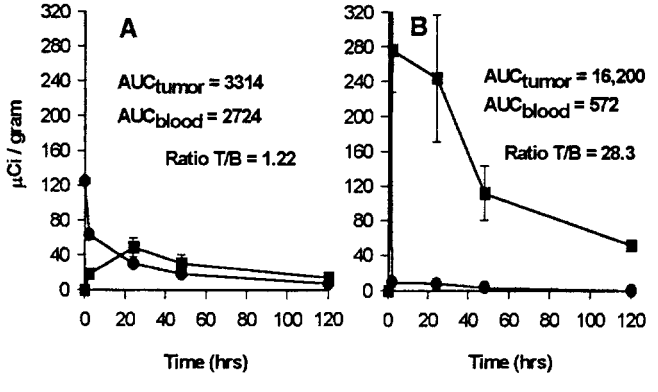

Fig. 3. Projected radioactivity concentrations resulting from either ^{90}Y-NR-LU-10 whole antibody or pretargeted ^{90}Y-DOTA-biotin. Tumor uptake (■) and blood clearance (●) data from Table 1 (mean %i.d./g of tissue) were used to calculate the decay-corrected radioactivity concentration after administration of either 200 μCi ^{90}Y-NR-LU-10 whole antibody (*A*) or 800 μCi pretargeted ^{90}Y-DOTA-biotin (*B*). Data are presented as μCi of ^{90}Y/g of tissue +/− SD at 2, 24, 48, and 120 hr postinjection. AUC values were calculated by using trapezoidal integration from 0 hr to 120 hr postinjection from the data in Table 1. T/B, tumor to blood.

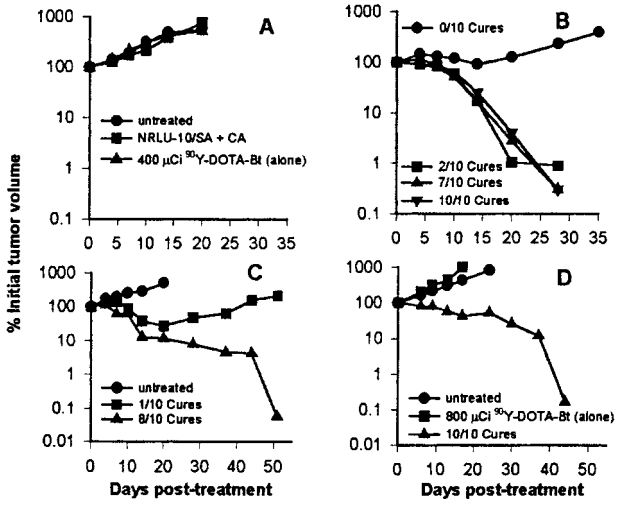

Fig. 4. Antitumor activity of pretargeted ^{90}Y-DOTA-biotin. Cure is defined as an established tumor that is not palpable for >300 days posttreatment. Data are presented as the average (10 animals/group) percent of initial tumor volume. (*A*) SHT-1 lung tumor xenografts (200–300 mm^3 at the initiation of therapy). Controls included untreated animals (●), and those treated with only NR-LU-10/SA plus CA (■), or given 400 μCi of nonpretargeted ^{90}Y-DOTA-biotin. (*B*) SHT-1 lung tumor xenografts (200–300 mm^3 at the initiation of therapy). Two hundred microcuries of ^{90}Y-NR-LU-10 whole antibody (100 μg) (●), 200 μCi (■), 400 μCi (▲), or 600 μCi (▼) of pretargeted ^{90}Y-DOTA-biotin. (*C*) MDA-MB-484 breast tumor xenografts 150–300 mm^3 at the initiation of therapy. Control animals (●), 200 μCi of ^{90}Y-NR-LU-10 whole antibody (100 μg) (■), or 800 μCi (▲) of pretargeted ^{90}Y-DOTA-biotin. (*D*) SW-1222 colon tumor xenografts 100–300 mm^3 at the initiation of therapy. Control animals (●), 800 μCi of nonpretargeted ^{90}Y-DOTA-biotin (■), and 800 μCi of pretargeted ^{90}Y-DOTA-biotin (▲).

as no tumor recurrence for at least 365 days, were also dose dependent with 2/10 at 200 μCi, 7/10 at 400 μCi, and 10/10 at 600 μCi. Tumors that initially regressed but later recurred showed an average growth delay of >50 days. Pretargeted treatment of mice bearing SHT-1 xenografts with a nonspecific, isotype-matched antibody/SA conjugate (NRML-05 antibody, targeting a 297-kDa melanoma-associated antigen not present in SHT-1 xenografts) and 400 μCi of ^{90}Y-DOTA-biotin produced only slight tumor growth suppression and no cures (data not shown). Immunohistology of recurrent tumors showed NR-LU-10 antigen expression remained at pretreatment levels. None of the control groups showed an effect (Fig. 4*A*). Therefore, antigen-specific, dose-dependent cures were achieved with a single dose of pretargeted ^{90}Y, but not by conventional RIT or by matched, nonspecific antibody-SA controls.

Similarly, treatment of MDA-MB-484 human breast tumors with 800 μCi of pretargeted ^{90}Y-DOTA-biotin produced a >90% tumor volume reduction resulting in 8/10 complete regressions that were also cures (Fig. 4*C*). The two tumors that recurred showed a growth delay of >60 days. Treatment with 200 μCi of ^{90}Y-DOTA-NR-LU-10 produced one cure, 60% partial regressions, and a growth delay of ≈35 days. Treatment of SW-1222 human colon tumors with 800 μCi of ^{90}Y-DOTA-biotin produced cures in all 10/10 animals (Fig. 4*D*). Conventional RIT had no impact on these tumors. Using the SW-1222 colon cancer xenograft as a model, we calculated the radiation dose delivered to these tumors. Assuming an absorbed fraction of 50% because of the long path length of ^{90}Y radiation and small diameter of xenografts (≈7 mm), estimates of the radiation dose to tumors with pretargeted ^{90}Y-DOTA-biotin were in excess of 15,000 cGy.

Hematologic Toxicity. Hematopoietic toxicity was measured in nontumored mice that received increasing doses of ^{90}Y delivered

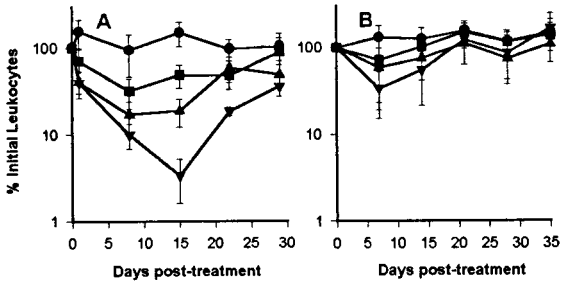

Fig. 5. Hematologic toxicity resulting from either ^{90}Y-NR-LU-10 whole antibody or pretargeted ^{90}Y-DOTA-biotin. Leukocyte toxicity was measured in separate groups of BALB/c female mice (n = 10) at weekly intervals postinjection. (*A*) On day −1, mice received (i.v.) either saline (●) or 100 μCi (■), 200 μCi (▲), or 300 μCi (▼) of ^{90}Y-NR-LU-10 whole antibody. (*B*) On day −1, mice received (i.v.) 400 μg NR-LU-10/SA, followed on day 0 by 200 μg of CA and either saline (●) or 200 μCi (■), 400 μCi (▲), or 800 μCi (▼) of pretargeted ^{90}Y-DOTA-biotin. Specific activities of radiolabeled reagents were varied, with total mass dose held constant. Data are presented as the mean ± SD percent of initial leukocyte values.

in either the pretargeted or conventional RIT formats. Blood was sampled weekly for leukocyte and platelet counts. Animals that received 100–300 μCi of ^{90}Y-DOTA-NR-LU-10 showed a dose-dependent nadir at 2 weeks in both platelet counts (11 ± 4% of initial at the 300 μCi dose) and leukocyte (Fig. 5*A*) counts (3.4 ± 1.8% of initial at the 300 μCi dose), with one death in the 300 μCi group. All animals that received 400 μCi of ^{90}Y-DOTA-NR-LU-10 died within 10 days of injection, presumably from acute hematologic toxicity. An estimation of 200 μCi as the MTD for ^{90}Y-DOTA-NR-LU-10 is consistent with the work of DeNardo *et al.* (33), who reported an LD_{50} of 307 μCi for an ^{90}Y-DOTA-whole antibody conjugate in a BALB/c mouse model.

By contrast, at doses up to 800 μCi, all animals that received pretargeted ^{90}Y-DOTA-biotin survived with no apparent sequelae. Animals that received either 400 or 800 μCi showed a dose-dependent nadir at 2 weeks for platelet counts (66 ± 26% of initial at the 800 μCi dose) and nadir at 1 week for leukocyte counts (34 ± 18% of initial counts at the 800 μCi dose, Fig. 5*B*). The MTD for pretargeted ^{90}Y in this animal model has not yet been determined.

Discussion

The pretargeting protocol and components described here constitute a RIT delivery strategy resulting in improved pharmacokinetics and enhanced therapeutic ratios and efficacy, with less toxicity, compared with directly radiolabeled whole antibody. In contrast to some other multistep delivery protocols and reagents (particularly bispecific antibody hybrids that possess monovalent binding for ligand/effector and antigen), the system reported here preserves divalent antibody-antigen interaction and tetravalent, ultra-high affinity ligand-receptor binding. This system affords flexibility in dosing and timing intervals, the ability to optimize biodistribution and tumor/normal organ ratios of radiation exposure over a broad range of ligand-chelate specific activities (μCi g^{-1}), and the preservation of the stable retention characteristics of whole antibody at the tumor target. Other approaches to reduce the toxicity of radiolabeled antibodies in conventional RIT have focused on using smaller antibody fragments to decrease the circulating half-life of the radiation, but the normal processing of these modified proteins generally has resulted in decreased delivery efficiency to tumor and increased kidney retention (34).

There are limitations in directly extrapolating these results to humans (e.g., expression of tumor target antigen in normal

human tissues, improved vascularity in s.c. animal tumor xenografts). However, this model has proved useful. Studies in mice with s.c. xenografts using ^{186}Re-NR-LU-10, for example, predicted the results with this agent in human clinical trials (17, 18). Tumor/blood ratios were similar and both exhibited the same dose-limiting and efficacy-limiting hematologic toxicity despite a nearly 10-fold higher concentration of hematopoietic stem cells in mice (35). Although animal xenografts exhibit a greater efficiency of tumor uptake of radiolabeled antibody than is typically seen in humans (30% i.d./g in mice versus 0.015% i.d./g in humans), a similar absolute concentration of radioactivity in μCi/g at the MTD has been observed (17, 18). Mouse xenograft studies are conservative predictors of human results when one considers the relatively long, 5-mm peak pathlength of the ^{90}Y β-emissions in relation to the size of the mouse and xenograft. Tumor dose is reduced by loss of absorbed dose, and toxicity could be enhanced through exposure to a greater volume of normal tissue.

Compared with carcinomas, lymphomas and leukemias generally provide better access to target antigen, and the circulating disease cells may experience direct cytotoxic effects via binding of whole antibodies. These qualities, along with the inherent radiosensitivity of hematologic malignacies, have made clinical RIT of lymphomas one of the few applications with established clinical efficacy (36–38). Yet, in the absence of bone marrow support, RIT of lymphomas is radiation dose-limited by hematologic toxicity, limiting therapeutic efficacy. Given the steep dose-response curve of these diseases, this effective application of conventional RIT could potentially benefit from a pretargeting approach as well.

In summary, the swift tumor uptake and stable retention of biotin-radionuclide, together with its extremely rapid blood and whole body clearance, resulted in a >20-fold improvement in tumor-to-blood AUC ratios over conventional RIT. Corresponding improvement of therapeutic ratios to all measured normal organs and tissues also was noted. The improvement was achieved through both decreased blood exposure and increased absolute dose (and dose rate) to tumor. These effects have been directly translated into improved efficacy (28/30 cures vs. 1/30 cures) and safety (MTD >800 μCi vs. MTD $\approx$200 μCi) of pretargeting compared with conventional RIT. Despite the rapid whole body clearance of the small radiobiotin molecule, there was no decrease in delivery efficiency (% i.d./g). This system allows the safe use of large doses of high-energy, short half-life radionuclides, enhances their antitumor efficacy through more rapid localization at the tumor, and permits increased absolute dose and dose rate to tumor compared with conventional RIT. Tests of second-generation reagents will assess potentially enhanced performance, increased dosing flexibility, greater chemical definition, easier manufacture, incorporation of antibodies with less normal human tissue reactivity, and decreased potential for immunogenicity.

We thank Gina Engrissei for care of the animals, Nicholas Raineri for the histological studies, as well as Dr. David Goodwin and Dr. Claude Meares for helpful scientific discussion. The communicating member is a member of the Scientific Advisory Board of Neutron Therapies, Inc.

1. Langmuir, V. K. (1992) *Nucl. Med. Biol.* **19,** 213–225.
2. Vittetta, E. S., Fulton, R. J., May, R. D., Till, M. & Uhr, J. W. (1987) *Science* **238,** 1098–1104.
3. Trail, P. A., Willner, D., Lasch S. J., Henderson, A. J., Hofstead, S., Casazza, A. M., Firestone, R. A., Hellstrom, I. & Hellstrom, K. E. (1993) *Science* **261,** 212–215.
4. Mello, A. M., Pauwels, E. K. J. & Cleton, F. J. (1994) *J. Cancer Res. Clin. Oncol.* **120,** 121–130.
5. Jain, R. K. (1994) *Sci. Am.* **271,** 58–65.
6. Cassidy, J., Newell, D. R., Wedge, S. R. & Cummings, J. (1993) *Cancer Surv.* **17,** 315–341.
7. Reilly, R. M., Sandhu, J., Alvarez-Diez, T. M., Gallinger, S., Kirsh, J. & Stern, H. (1995) *Clin. Pharmacokinet.* **28,** 126–142.
8. Knox, S. J. (1995) *Cancer Res.* **55,** 5832s–5836s.
9. Paganelli, G., Malcovati, M. & Fazio, F. (1991) *Nucl. Med. Commun.* **12,** 211–234.
10. LeDoussal, J. M., Martin, M., Gautherot, E., Delaage, M. & Barbet, J. (1989) *J. Nucl. Med.* **30,** 1358–1366.
11. Stickney, D. R., Anderson, L. D., Slater, J. B., Ahlem, C. N., Kirk, G. A., Schweighardt, S. A. & Frincke, J. M. (1991) *Cancer Res.* **51,** 6450–6655.
12. Kalafonos, H. P., Ruskowski, M., Siebecker, D. A, Sivolapenko, G. B., Snook, D., Lavender, J. P., Epenetos, A. A. & Hanatowich, D. J. (1990) *J. Nucl. Med.* **31,** 1791–1796.
13. Goodwin, D. A., Meares, C., Diamanti, C., McCall, M., Lai, C., Torti, F., McTigue, M. & Martin, B. (1984) *Eur. J. Nucl. Med.* **9,** 209–215.
14. Goodwin, D. A., Meares, C. & McCall, M. (1989) U.S. Patent Number 4,863,713.
15. Okabe, T., Kaizu, T., Fujisawa J., Watanabe, J., Kojima, K., Yamashita, T. & Takaku, F. (1984) *Cancer Res.* **44,** 5273–5278.
16. Litvinov, S. V., Velders, M. P., Bakker, H. A. M., Fleuren, G. J. & Warnaar, S. O. (1994) *J. Cell Biol.* **125,** 437–446.
17. Beaumier, P. L., Venkatesan, P., Vanderheyden, J.-L., Burgua, W. D., Kunz, L. L., Fritzberg, A. R., Abrams, P. G. & Morgan, A. C. (1991) *Cancer Res.* **51,** 676–681.
18. Breitz, H. B., Weiden, P. W., Vanderheyden, J.-L., Appelbaum, J. W., Bjorn, M. J., Fer, M. F., Wolf, S. B., Ratliff, B. A., Seiler, C. A., Foisie, D. C., *et al.* (1992) *J. Nucl. Med.* **33,** 1099–1109.
19. Graves, S. S., Goshorn, S. C., Stone, D. M., Axworthy, D. B., Reno, J. M., Bottino, B., Searle, S., Henry, A., Pedersen, J., Rees, A. R. & Libby, R. T. (1999) *Clin. Cancer Res.* **5,** 899–908.
20. Janolino, V. G., Fontecha, J. & Swaisgood, H. E. (1996) *Appl. Biochem. Biotech.* **56,** 1–7.
21. Wilbur, D. S., Hadley, S. W., Hylarides, M. D., Abrams, P. G., Beaumier, P. L., Morgan, A. C., Reno, J. M. & Fritzberg, A. R. (1989) *J. Nucl. Med.* **30,** 216–226.
22. Lee, Y. C., Stowell, C. P. & Krantz, M. J. (1976) *Biochemistry* **15,** 3956–3963.
23. Viles, F. J., Jr. & Silverman, L. (1949) *Anal. Chem.* **21,** 950–953.
24. Axworthy, D. B., Theodore, L. J., Gustavson, L. M. & Reno, J. M. (1997) U.S. Patent 5,608,060.
25. Mock, D. M. & DuBois, D. B. (1986) *Anal. Biochem.* **153,** 272–278.
26. Ruskowski, M., Fogarasi, M., Fritz, B. & Hnatowich, D. J. (1997) *Nucl. Med. Biol.* **24,** 263–268.
27. Green, N. M. (1990) *Methods Enzymol.* **184,** 51–67.
28. Schecter, B., Arnon, R., Colas, C., Burakova, T. & Wilchek, M. (1995) *Kidney Int.* **47,** 1327–1335.
29. Schecter, B., Silberman, R., Arnon, R. & Wilchek, M. (1990) *Eur. J. Biochem.* **189,** 327–331.
30. Weigel, P. H. (1992) in *Glycoconjugates: Composition, Structure and Function*, eds. Allen, H. J. & Kisailus, E. C. (Dekker, New York), pp. 421–497.
31. Meares, C. F., Moi, M. K., Diril, H., Kukis, D. L., McCall, M. J., Deshpande, S. V., DeNardo, S. J., Snook, D. & Epenetos, A. A. (1990) *Br. J. Cancer* **62**, Suppl., 21–26.
32. Craft, D. V., Goss, N. H., Chandramouli, N. & Wood, H. G. (1985) *Biochemistry* **24,** 2471–2476.
33. DeNardo, G. L., Kroger, L. A., DeNardo, S. J., Miers, L. A., Salako, Q., Kukis, D. L., Fand, I., Shen, S., Renn, O. & Meares, C. F. (1994) *Cancer* **73,** 1012–1022.
34. Rowlinson-Busza, G., Deonarian, M. P. & Epenetos, A. A. (1996) *Tumor Targeting* **2,** 37–48.
35. Hall, E. J. (1994) *Radiobiology for the Radiologist* (Lippincott, Philadelphia), pp. 317–318.
36. Press, O. W., Eary, J. F., Applebaum, F. R., Martin, P. J., Badger, C. C., Nelp, W. B., Glenn, S., Butchko, G., Fisher, D. & Porter, B. (1993) *N. Eng. J. Med.* **329,** 1219–1224.
37. Kaminsky, M. S., Zasadny, K. R., Francis, I. R., Milik, A. W., Ross, C. W., Moon, S. D., Crawford, S. M., Burgess, J. M., Petry, N. A. & Butchko, G. M. (1993) *N. Eng. J. Med.* **329,** 459–465.
38. Knox, S. J., Goris, M. L., Trisler, K., Negrin, R., Davis, T., Liles, T. M., Grillo-Lopez, A., Chinn, P., Varns, C., Ning, S. C., *et al.* (1996) *Clin. Cancer Res.* **2,** 457–470.